Malaysian Journal of Chemistry, 2026, Vol. 28(1), 453-460
(Special Issue: *12th International Conference of the College of Science & 3rd Conference of Chemistry Department 2025*)

DFT-Based Theoretical Study of Structural, Stability, Electronic, and Thermodynamic Properties of Nitrogen Doped Graphene-TiO_2 Heterostructure

Worood S. Rasool, M. A. AL-Kaabi*, Nibras Mossa Umran and Qasim Hassan Ubaid
Department of Physics, College of Science, Kerbala University, Karbala, Iraq
*Corresponding author (e-mail: mohammed.alkaabi@uokerbala.ed.iq)

This study investigates the structural, stability, electronic, and thermodynamic properties of nitrogen-doped graphene (NGR) integrated with titanium dioxide (TiO_2). The NGR/TiO_2 heterostructure consists of 98 atoms (47 carbon, 32 oxygen, and 16 titanium) with three nitrogen doping sites. Comprehensive analysis reveals a minimum separation of 3 Å between TiO_2 and NGR, with a formation energy of -5.47 eV, indicating weak van der Waals interactions rather than covalent bonding. The optimized structure exhibits exceptional stability, as validated by phonon dispersion spectra that are devoid of imaginary frequencies. Electronic band structure calculations reveal the absence of an energy gap, which enhances electrical conductivity and photocatalytic performance, attributed to N-induced states near the Fermi level. Nitrogen dopants tend to acquire negative charges, which is consistent with their elevated electronegativity in comparison to carbon, thereby facilitating the attraction of electron density. These findings suggest that modifying NGR/TiO_2 with dopants can improve interfacial interactions, paving the way for advanced applications in energy storage and photocatalysis.

Keywords: Density Functional Theory, interface, band structures, phonon dispersion

Received: October 2025; Accepted: November 2025

Semiconductor photocatalysis is recognized as an auspicious methodology to concurrently mitigate energy demands and environmental contamination. TiO_2 has been extensively examined for such purposes owing to its cost-effectiveness, non-toxic nature, and remarkable chemical stability. Nevertheless, pristine TiO_2 continues to experience challenges related to its inadequate utilization of visible light and a pronounced rate of photogenerated charge-carrier recombination [1]. Moreover, it exhibits diminished photocatalytic efficacy under visible-light irradiation and a limited light response spectrum due to its inherently wide band gap [2].

The incorporation of graphene onto n-type semiconductor photocatalysts facilitates the direct migration of photogenerated electrons from the semiconductor to graphene [3]. Consequently, a substantial number of scholarly articles elucidate the findings of investigations concerning the modifications of starting materials via metal or non-metal ions, or the coupling of TiO_2 with alternative semiconductors, particularly aimed at producing visible-light-driven photocatalysts characterized by enhanced photoactivity and mitigated charge carrier recombination [4]. Notably, various design methodologies, including the doping and sensitization of semiconductors with graphene, enhancement of graphene electrical conductivity, augmentation of electrocatalytic active sites on graphene, fortification of interface coupling between semiconductors and graphene, fabrication of micro/nano architectures, construction of multi-junction nanocomposites, improvement of semi-conductors' photostability, and the employment of synergistic effects from diverse modification strategies, are comprehensively summarized [5].

Typically, the photocatalytic efficacy of TiO_2 is significantly contingent upon its phase structure, crystallite dimensions, specific surface area, and pore architecture [6]. Charge carriers are generated on the catalyst's surface when it is exposed to ultraviolet or visible light. Due to the advantageous position of the Fermi level, the valence band (VB) holes of aromatic graphene diminish electron recombination when photoelectrons are transferred from the conduction band (CB) of TiO_2. In this context, graphene-based materials serve as electron reservoirs. When the electrons present on the surface of carbon-based graphene materials interact with adsorbed or dissolved oxygen, superoxide radicals are generated. These radicals play a critical role in photocatalytic processes [7]. The incorporation of heteroatom-doped nanocomposites results in an enhancement of the overall desirable characteristics of novel synthesized materials for the sensing of various analytes of interest. Among the heteroatoms, the doping of nitrogen (N) is particularly noteworthy due to its electron-rich characteristics, comparable atomic size to carbon, and substantial electronegativity, which may provide a suitable site for incorporation into the graphene lattice [8].

†Paper presented at the 12th International Conference of the College of Science & 3rd Conference of Chemistry Dept. 2025

In this study, we investigate the interactions between NGR/TiO_2 materials utilizing density functional theory (DFT)-based calculations, facilitating the optimization of structural stability and the prediction of bandgap behavior. This understanding lays the foundation for the advancement of superior materials and devices with enhanced performance across a spectrum of applications. The amalgamation of TiO_2 with graphene presents significant promise, and through DFT analysis, we can unveil their synergistic potential and open new avenues within the realms of materials science and technology.

THEORETICAL

Density Functional Theory

The density functional theory (DFT) calculations were conducted utilizing a plane-wave-basis methodology as integrated within the computational framework of CASTEP (Cambridge Sequential Total Energy Package), a well-recognized first-principles computational instrument predicated on plane-wave pseudopotential techniques [9]. For the exchange-correlation potential, the Perdew-Burke-Ernzerhof (PBE) generalized gradient approximation (GGA) exchange-correlation functional was employed [10]. Given the inadequacy of GGA to accurately characterize the on-site Coulomb interaction between localized d and f electrons, we implemented DFT+U to address the localized 3d electrons in pursuit of obtaining more authentic electronic properties. A correction of Ueff = 4.5 eV (U = 4.5, J = 0) [11]. It was incorporated in accordance with the methodology proposed by Dudarev [12]. Van der Waals interactions between TiO_2 and doped graphene were incorporated utilizing the DFT-D2 by Tkatchenko and Scheffler [13]. A kinetic energy cutoff of 750 eV was utilized to encompass plane waves within the basis set. The constructed geometric configuration was optimized until the total energy and force per atom were reduced to less than 10^{-6} eV and 0.001 eV Å-1, with a maximum displacement of 0.001 Å and a maximum stress of 0.05 GPa for the NGR/TiO_2 bilayer. The integrations over the first Brillouin zone were performed employing a grid of 3x3x2 points within the NGR/TiO_2 system during the geometry optimization process. We subsequently assessed charge transfer phenomena through differential charge density analysis.

The lattice mismatch in the x- and y-directions was computed based on the lattice parameters of TiO_2 and N-GR monolayer, respectively. This computation yielded a lattice mismatch of 4.05%. Moreover, we established a vacuum spacing exceeding 20 Å to mitigate interactions among the heterostructures of adjacent layers within the periodic slabs [14].

The NGR monolayer comprised 47 carbon and three nitrogen atoms within the supercell. The TiO_2 monolayer incorporates a total of 48 atoms, consisting of 32 oxygen atoms and 16 titanium atoms, within a supercell. Figure 1 illustrates the entirety of the NGR/TiO_2 bilayer, which encompasses a total of 98 atoms.

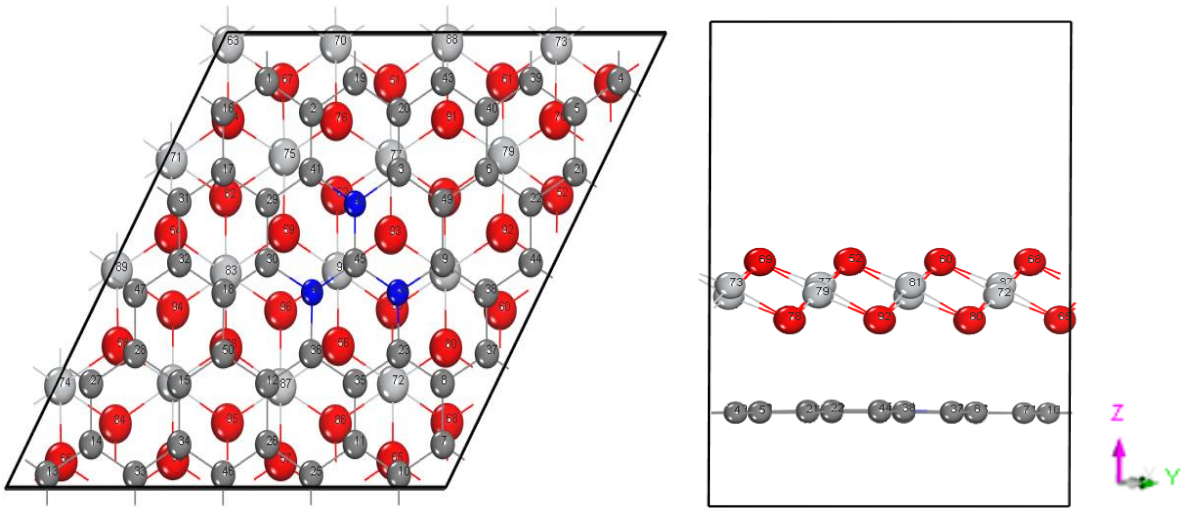

Figure 1. Side (a) and top view (b) of the NGR/TiO_2.

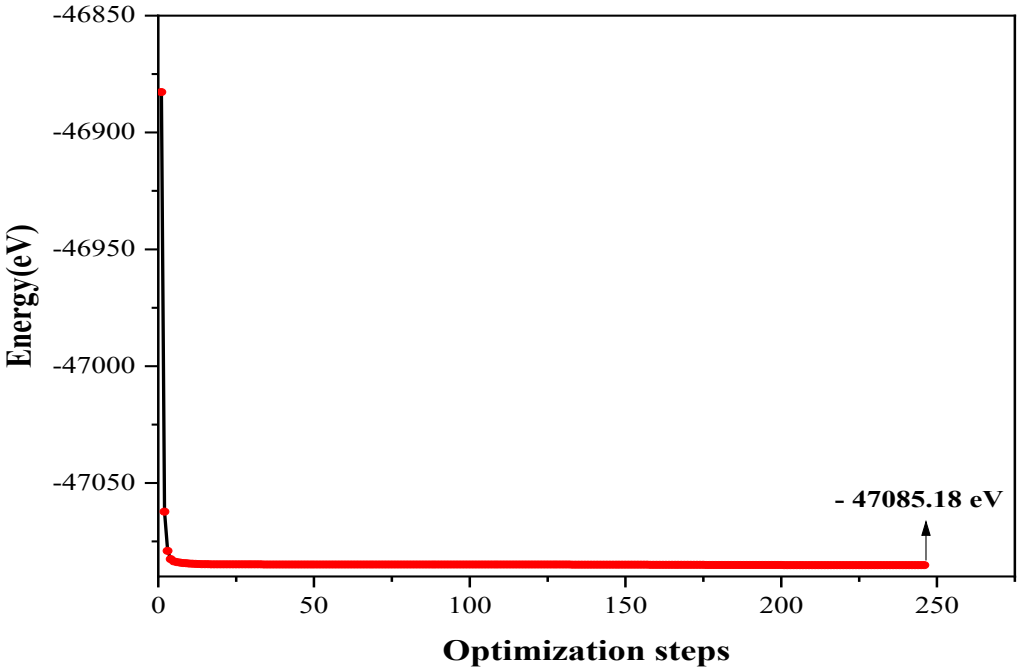

Figure 2. Optimization of the energy of NGR/TiO2.

RESULTS AND DISCUSSION

Formation Energy of the NGR/TiO_2

Doping with electron-donor nitrogen heteroatoms can effectively modulate the electronic characteristics of graphene, yielding an n-type semiconductor [15].

Primarily, an NGR/TiO_2 bilayer composed of 98 atoms (47 carbon atoms, 32 oxygen atoms, and 16 titanium atoms) is doped with three nitrogen atoms, resulting in a nitrogen concentration of 3.06% within the host NGR/TiO_2 bilayer.

Additionally, we present comprehensive data regarding the minimum (dmin) and average (dav) distances between the doped graphene (NGR) sheet and the bridging oxygen (O) atoms situated at the titania surface, in conjunction with the formation energy, which delineates the energetic disparity between the isolated NGR and the TiO_2slab models.

The comprehensive energy of the system exhibits a declining trend as the volume increases, ultimately achieving a minimum that corresponds to the ground state. (Figure 2) illustrates the minimum energy, quantified as (-47085.18 eV). The optimized lattice parameters were determined as a=12.194 Å, b=12.190 Å, and c=15.83 Å.

The interfacial region between the NGR/TiO_2 is predominantly influenced by weak dispersion forces. The minimum separation distance recorded between an atom of the adsorbed TiO_2 and the nearest carbon atom of the NGR/TiO_2 bilayer is 3 Å, accompanied by a formation energy of -5.47 eV per supercell, compared with the theoretical study [16]. Chemical doping with nitrogen exhibits a relatively negligible impact on both the equilibrium distance and the binding energy. The planar configuration of the graphene surface suggests the predominance of van der Waals forces over covalent bonding at the interface [17].

The considerable separation between the layers discussed attenuates the anticipated synergistic effects, thereby constraining the enhancement of the material properties. Furthermore, in light of preceding experimental studies, it can be asserted that graphene is a material that exhibits a reluctance to react with TiO_2; thus, in applications involving nanocomposites, it is imperative to modify its structure through the introduction of dopants and oxygenated functional groups that facilitate layer anchoring. These findings also present avenues for alternative methodologies, such as incorporating interlayers to promote more robust interactions and connections. The lattice mismatch between NGR and TiO_2 monolayers is a mere 4.7%. Upon the conclusion of the geometry optimization process, the carbon (C) atom layers across all composites remain planar, reinforcing the assertion that the type of interaction existing between NGR and TiO_2 is characterized by van der Waals forces, rather than covalent interactions. This observation aligns well with other computational results [18]. The energy of the doped graphene is measured at -8031.95 eV.

Structural Properties

The optimized NGR/TiO_2 bilayer demonstrates exceptional structural properties, as substantiated by the phonon dispersion spectra, which exhibit an absence of imaginary frequencies. This suggests that the system maintains dynamic stability at 0 K. Conversely, the incorporation of nitrogen atoms introduces localized bonding sites that enhance interfacial coupling. In comparison to other molecular parameters, bond lengths are likely instrumental in the classification of chemical bonds [19]. The results correlate with both experimental and theoretical values in a reliable manner [20-21], revealing that the properties examined indicate that the C-C and C-N ring bonds are characteristic of covalent interactions.

Bond length analysis yields additional insights. The C–N bonds present within the nitrogen-doped graphene layer are determined to range between 1.371 and 1.426 Å, values that are in proximity to previously established theoretical estimations for pyridinic and graphitic nitrogen (approximately 1.39–1.40 Å) [21]. These marginal discrepancies, when contrasted with pristine C–C bonds (approximately 1.40–1.41 Å), signify the modified electronic environment engendered by substitutional doping.

Stability and Thermodynamic Properties

The phonon dispersion curve further validates the dynamic stability of the system [22]. The absence of negative phonon frequencies over the entire Brillouin zone (see Figure 3) attests to the intrinsic stability of the materials. Phonon density of states (PhDOS) calculations elucidates contributions from both NGR and TiO_2 vibrational modes (see Figure 4). The maintenance of acoustic modes corroborates mechanical integrity, while the shifts observed in high-frequency optical modes reflect C–N vibrational contributions, aligning with prior investigations on doped graphene/TiO_2 systems [23].

Thermodynamic properties such as heat capacity, entropy, enthalpy, and Helmholtz free energy exhibit anticipated trends with ascending temperature. Specifically, heat capacity converges towards the Dulong–Petit limit at elevated temperatures, whereas the continuous increase of entropy and enthalpy signifies the thermodynamic favorability of the doped system. The decline in Helmholtz free energy at increased temperatures further substantiates enhanced stability under thermal excitation (Figure 5). These behaviors are consistent with previous theoretical studies on graphene/oxide heterostructures [24], which underscored the role of phonon-driven stabilization as a crucial factor for applications in energy storage and photocatalysis.

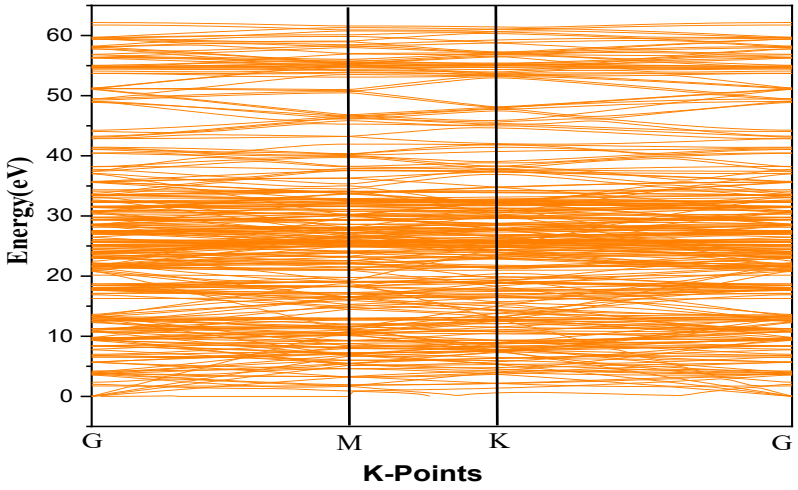

Figure 3. The phonon dispersion for NGR /TiO_2 using DFPT.

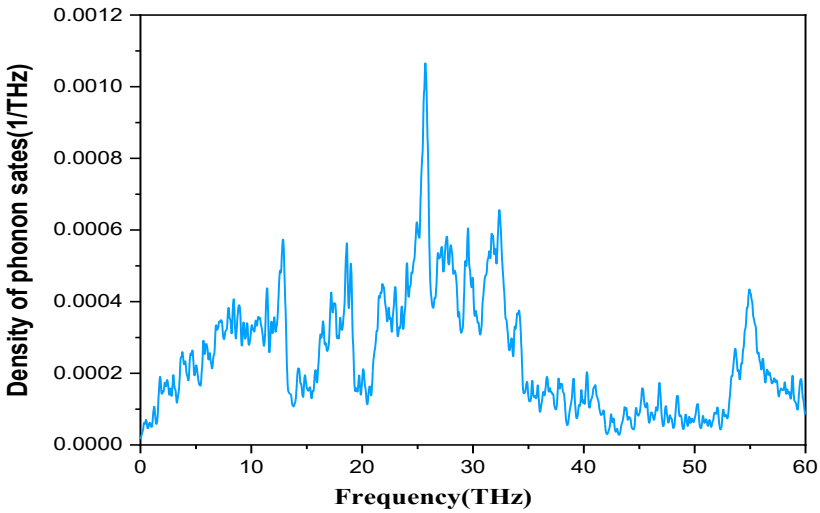

Figure 4. The density of phonon state curves for NGR /TiO_2 using DFPT.

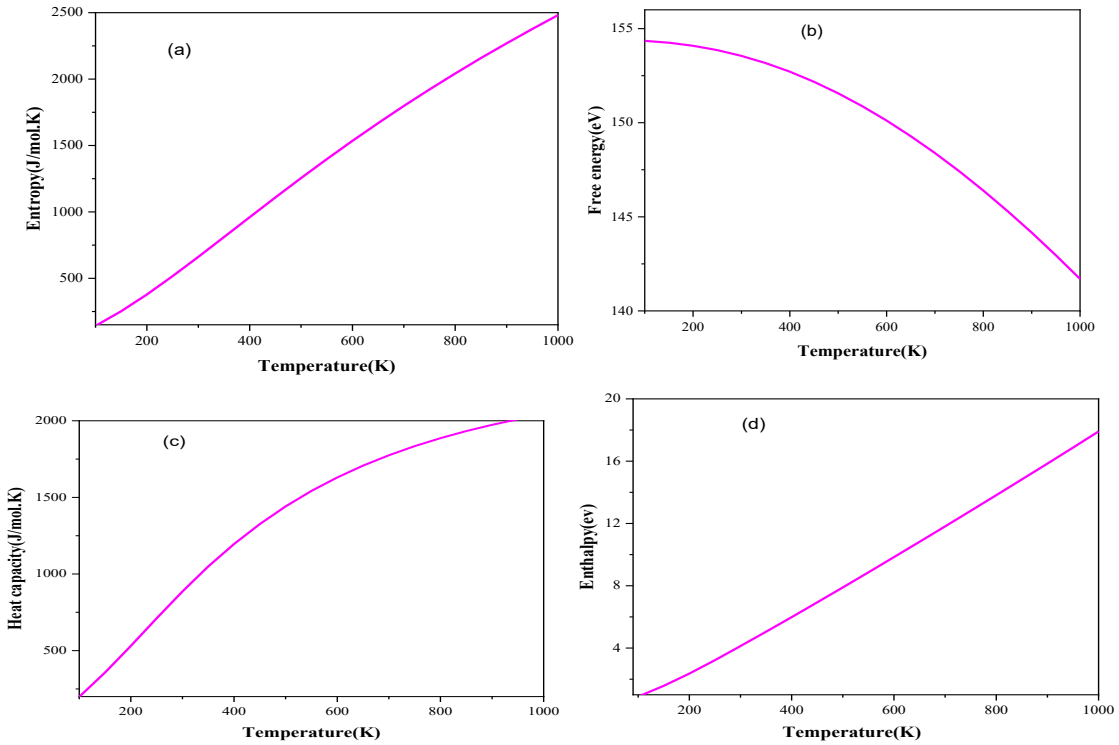

Figure 5. (a) Entropy, (b) free energy, (c)heat capacity, and(d) enthalpy for NGR /TiO_2.

Electronic Structures

To evaluate the impact of hybridization on the electronic properties of the NGR/TiO_2 bilayer, electronic band structures were computed, as depicted in Figure 6(a). The band gaps were assessed using the GGA-PBE+U functional, focusing on high-symmetry points in the Brillouin zone (G-M-K-G). The maximum of the valence band (VB) is situated between the M and K points, while the minimum of the conduction band (CB) is found at the Γ point. Analysis of the projected density of states (PDOS) supports this observation, highlighting the formation of N-induced states near the Fermi level, which effectively reduces the bandgap of the heterostructure. This noticeable decrease in bandgap correlates with a significant enhancement in electrical conductivity, as corroborated by several experimental studies [25,26]. The lower bandgap of the NGR/TiO_2 composite facilitates electronic transitions between the VB and CB, which

contributes to its superior photocatalytic performance compared to the TiO_2 monolayer. The Fermi level is set to zero, and the band gap is equal to 0eV. In the NGR/TiO_2 bilayer, efficient separation of charge carriers (electrons and holes) suggests improved photocatalytic activity relative to the TiO_2 monolayer. The indirect bandgap nature in NGR/TiO_2 promotes reduced recombination of excited electron-hole pairs due to differences in k-space momentum. A thorough examination of the electronic structure of TiO_2 and the NGR/TiO_2 heterostructure reveals that the formation of this heterostructure, held together by van der Waals forces, leads to a significant low-energy shift in the PDOS of TiO_2, indicating a crucial alteration in its electronic properties. The upper valence band primarily comprises C 2p and O 2p states, with a notable dominance of O 2p orbitals, reflecting a substantial localization of electronic charge around the oxygen atoms. Strong hybridization among C 2p, O 2p, and Ti 3d orbitals is observed in the lower conduction band. This hybridization is further confirmed by the PDOS analysis shown in (Figure 6b), which reveals significant contributions from interfacial oxygen atoms in the upper occupied states of the valence band, resulting from van der Waals interactions between oxygen and carbon atoms in graphene. Experimentally, the presence of oxygen at the interface is known to be vital for improving electron-hole separation, thereby enhancing the catalytic efficiency of the NGR/TiO_2 composite [27-29].

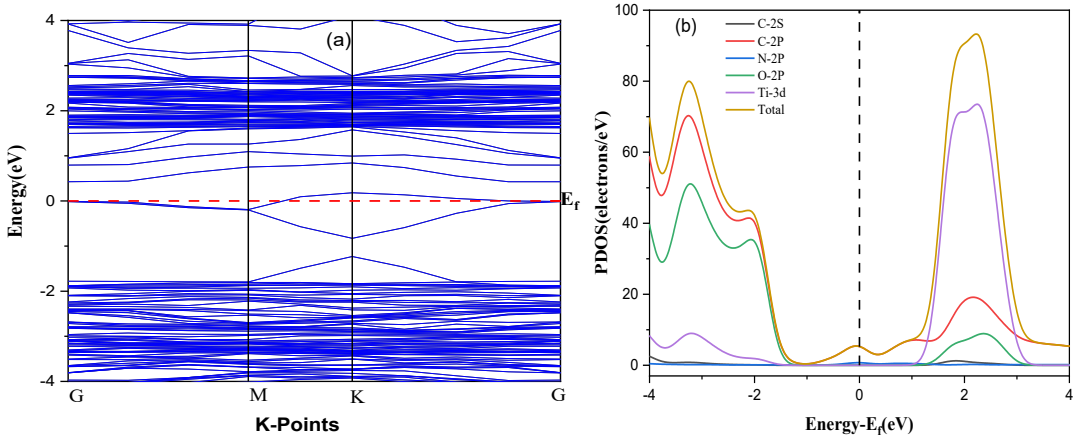

Figure 6. (a) The band structures and (b) PDOS for NGR /TiO_2.

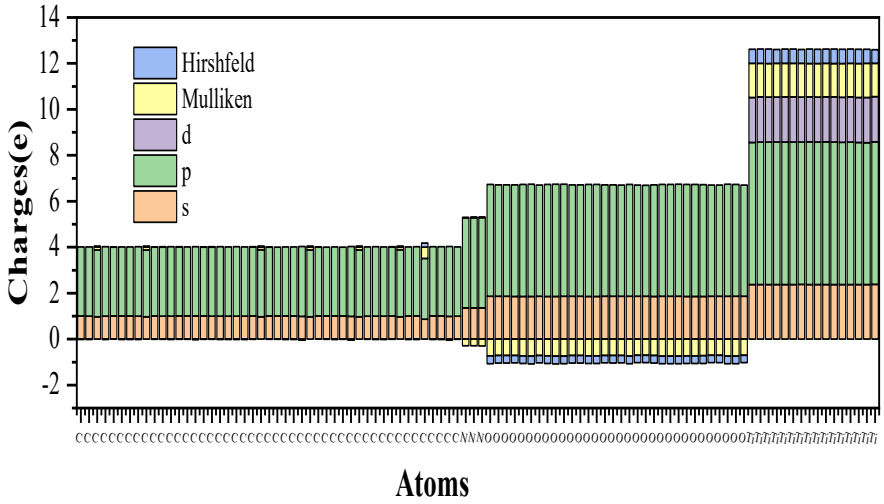

Figure 7. Atomic charges for NGR /TiO_2.

Atomic Charges

Atomic charges, utilizing both Mulliken and Hirshfeld methods, reveal significant redistribution of electronic density at the NGR/TiO_2 interface. Nitrogen dopants tend to acquire negative charges (–0.28 to –0.29 e), which is consistent with their elevated electronegativity in comparison to carbon, thereby facilitating the attraction of electron density. This phenomenon promotes interfacial charge transfer towards the titanium atoms, which display partial positive charges of up to +1.47 e, while the oxygen atoms maintain strongly negative values (–0.70 to –0.74 e) (Figure 7).

CONCLUSION

In conclusion, the integration of NGR with TiO_2 demonstrates significant enhancements in formation energy, structural stability, electronic, and thermodynamic properties. The presence of nitrogen dopant induces favorable electronic modifications, resulting in reduced bandgap and enhanced electrical conductivity. The weak van der Waals interactions at the NGR/TiO_2 interface, coupled with the effective charge transfer dynamics, underline the importance of doping in optimizing the performance of graphene-based nanocomposites. Furthermore, the findings highlight the necessity for structural modifications, such as doping and functionalization, to strengthen interfacial interactions and promote the catalytic efficiency of these materials. Overall, this research provides valuable insights into the potential applications of NGR/TiO_2 in energy storage and photocatalysis, paving the way for future advancements in nanomaterial design.

REFERENCES

1. Meng, A., Zhang, L., Cheng, B.and Yu, J. (2019). Dual cocatalysts in TiO2 photocatalysis. *Advanced Materials*, **31(30)**, 1807660.

2. Chen, J., Qiu, F., X,u W., Cao, S. and Zhu, H. (2015) Recent progress in enhancing photocatalytic efficiency of TiO2-based materials. *Applied Catalysis A: General*, **495**, 131–140.

3. Wang, L., Zhu, B., Cheng, B., Zhang, J., Zhang, L., and Yu, J. (2021). In-situ preparation of TiO_2/N-doped graphene hollow sphere photocatalyst with enhanced photocatalytic CO_2 reduction performance. *Chinese Journal of Catalysis*, **42(10)**, 1648–1658.

4. Kusiak-Nejman, E. and Morawski, A. W. (2019) TiO_2/graphene-based nanocomposites for water treatment: A brief overview of charge carrier transfer, antimicrobial and photocatalytic performance. *Applied Catalysis B: Environmental*, **253**, 179–186.

5. Li, X., Yu, J., Wageh, S., Al-Ghamdi, A., and Xie, J. (2016) Graphene in photocatalysis: a review. *Small*, **12(48)**, 6640–6696.

6. Zhang, J., Zhou, P., Liu, J. and Yu, J. (2014) New understanding of the difference of photocatalytic activity among anatase, rutile and brookite TiO_2, *Physical Chemistry Chemical Physics*, **16(38)**, 20382–20386.

7. Shaik, B. B., Katari, N. K., Raghupathi, J. K., Jonnalagadda, S. B., and Rana, S. (2024). Titanium Dioxide/Graphene-Based Nanocomposites as Photocatalyst for Environmental Applications: A Review. *ChemistrySelect*, **9(46)**, e202403521.

8. Patil, P. O., Nangare, S. N., Patil, P. P., Patil, A. G., Patil, D. R., Tade, R. S., Patil, A. M., Deshmukh, P. K., and Bari, S. B. (2021). Fabrication of N-doped graphene/TiO_2 nanocomposites for its adsorption and absorbing performance with facile recycling, **13**, 179–190.

9. Segall, M., Lindan, P. J., Probert, M. A., Pickard, C. J., Hasnip, P. J., Clark, S., and Payne, M. (2002). First-principles simulation: ideas, illustrations, and the CASTEPcode. *Journal of Physics: Condensed Matter* **14(11)**, 2717.

10. Perdew, J. P., Burke, K., and Ernzerhof, M. (1996). Generalized gradient approximation made simple. *Physical Review letters*, **77(18)**, 3865.

11. Blöchl, P. E. (1994) Projector augmented-wave method. *Physical Review Physical Review B*, **50(24)**, 17953.

12. Datteo, M. (2020) Quantum Chemical modelling of physical and chemical properties of TiO_2 hybrid interfaces between a semiconducting oxide surface and carbon-based layer.

13. Dudarev, S. L., Botton, G. A., Savrasov, S. Y., Humphreys, C., and Sutton, A. P. (1998) Electron-energy-loss spectra and the structural stability of nickel oxide: An LSDA+ U study. *Physical Review B*, **57(3**), 1505.

14. Tkatchenko, A. and Scheffler, M. (2009) Accurate molecular van der Waals interactions from ground-state electron density format and free-atom reference data. *Physical Review Letters*, **102(7)**, 073005.

15. Xuan, W., Yang, N., Luo, J., Wang, R., Yang, H., and Jin, G. (2023). Strain-modulated Rashba spin splitting and optical absorption of MoSSe/WSe2 heterostructures. *Applied Physics A*, **129(2)**, 88.

16. Jin, Z., Yao, J., Kittrell, C., and Tour, J. M. (2011) Large-scale growth and characterizations of

nitrogen-doped monolayer graphene sheets. *ACS Nano*, **5(5)**, 4112–4117.

17. Ferrighi, L., Datteo, M., Fazio, G., and Di Valentin, C. (2016) Catalysis under cover: enhanced reactivity at the interface between (doped) graphene and anatase TiO_2. *Journal of the American Chemical Society*, **138(23)**, 7365–7376.

18. Tsai, J. -L. and Tu, J. -F. (2010) Characterizing mechanical properties of graphite using molecular dynamics simulation. *Materials & Design*, **31(1)**, 194–199.

19. Xu, P., Tang, Q. and Zhou, Z. (2013) Structural and electronic properties of graphene–ZnO interfaces: dispersion-corrected density functional theory investigations. *Nanotechnology*, **24(30)**, 305401.

20. Lide Jr, D. R. (1962) A survey of carbon-carbon bond lengths. *Tetrahedron*, **17(3-4)**, 125–134.

21. Rani, P. and Jindal, V. (2013) Designing band gap of graphene by B and N dopant atoms. *RSC Advances*, **3(3)**, 802–812.

22. Biby, A. (2021). Nanoengineered Materials for Energy Conversion & Storage Applications: A Density Functional Theory Study.

23. Takahashi, N., Yoon, D. Y., and Parrish, W. (1984). Designing band gap of graphene by B and N dopant atoms. *Macromolecules*, **17(12)**, 2583–2588.

24. Shan, S., Liu, W., Zou, W., Chen, R., and Hu, C. (2024). The Effect of Vibration Frequency on the Effective Mass Spin Splitting of a Polaron in a Parabolic Quantum Well. *Acta Physica Polonica A ISSN 1898-794X*, **145(4)**, 157–157.

25. Narayan, J. and Bezborah, K. (2024). Recent advances in the functionalization, substitutional doping, and applications of graphene/graphene composite nanomaterials. *RSC Advances*, **14(19)**, 13413–13444.

26. Vempati, S. and Uyar, T. (2014) Fluorescence from graphene oxide and the influence of ionic, π–π interactions and heterointerfaces: electron or energy transfer dynamics. *Physical Chemistry Chemical Physics*, **16(39)**, 21183–21203.

27. Mori-Sánchez, P., Cohen, A. J., and Yang, W. (2008). Localization and Delocalization Errors in Density Functional Theory Format and Implications for Band-Gap Prediction. *Physical Review Letters*, **100(14)**, 146401.

28. Sham, L. J. and Schlüter, M. (1983) Density-functional theory of the energy gap. *Physical Review Letters*, **51(20)**, 1888.

29. Umrao, S., Abraham, S., Theil, F., Pandey, S., Ciobota, V., Shukla, P., Rupp, C. J., Chakraborty, S., Ahuja, R. and Popp, J. (2014) A possible mechanism for the emergence of an additional band gap due to a Ti–O–C bond in the TiO_2–graphene hybrid system for enhanced photodegradation of methylene blue under visible light. *RSC Advances*, **4(104)**, 59890–59901.